LA-UR- 09-01159

Approved for public release; distribution is unlimited.

Title: Application of X-Ray Tomography to the Optimization of new NOx/NH3 Mixed Potential Sensors for Vehicle On-board Emissions Control

Author(s): Mark A. Nelson, Eric L. Brosha, Todd Williamson, R. Mukundan, Fernando H. Garzon

Intended for: Electrochemical Society meeting, San Francisco, May 2008

Los Alamos
NATIONAL LABORATORY
EST. 1943

Form 836 (7/06)

Application of X-Ray Tomography to Optimization of New NO_x/NH_3 Mixed Potential Sensors for Vehicle On-board Emissions Control

M.A. Nelson (mnelson@lanl.gov), E.L. Brosha, T. Williamson, R. Mukundan, F.H. Garzon

Los Alamos National Laboratory, Sensors and Electrochemical Devices Group, Los Alamos, New Mexico, USA

Mixed potential sensors for the detection of hydrocarbons, NO_x, and NH_3 have been previously developed at Los Alamos National Laboratory (LANL). The LANL sensors have a unique design incorporating dense ceramic-pellet/metal-wire electrodes and porous electrolytes. The performance of current-biased sensors using an yttria-stabilized zirconia (YSZ) electrolyte and platinum and $La_{0.8}Sr_{0.2}CrO_3$ electrodes is reported. X-ray tomography has been applied to non-destructively exam internal structures of these sensors. NO_x and hydrocarbon response of the sensors under various bias conditions is reported, and very little NO_x response hysteresis was observed. The application of a 0.6 μA bias to these sensors shifts the response from a hydrocarbon response to a NOx response equal for both NO and NO_2 species at approximately 500 °C in air.

Over the past decade, Los Alamos National Laboratory (LANL) has developed a unique class of electrochemical gas sensors for the detection of carbon monoxide, hydrocarbons, hydrogen and nitrogen oxides.[1-9] These sensors are based on the mixed-potential phenomenon[10-14] and are a modification of the existing automotive lambda (oxygen) sensor and have the potential to meet the stringent sensitivity, selectivity and stability requirements of an on-board emissions/engine control sensor systems.

The use of High resolution X-ray Computed Tomography (XCT) [Xradia MicroXCT] to characterize NO_x/NH_3 sensors prepared by tape casting will be described. Mixed potential sensors have been produced in bulk, tape cast, and thin film variants for vehicle emissions control applications.[6,15–18] XCT imaging has the advantages in comparison to conventional SEM or TEM of being non-invasive, requiring little or no sample preparation, not damaging the sample, not requiring the sample to be conductive, and not disturbing the microstructure. Sensors produced with various sintering temperatures have been examined with XCT for cracking and other microstructural features and to gauge porosity, and some of these observations are presented with sensor performance data. We have shown in previous work that the response characteristics of mixed potential sensors is a function of density of the electrolyte and electrode materials. The porosity of the sensors is a function of firing schedule, (higher temperatures leading to higher density and lower porosity). XCT and ESEM are being used to perform a systematic study of the effect of sintering temperature and density on sensor response. These techniques have also been used to study the quality of the electrode-electrolyte interface.

The current state of the art LANL technology is based on the stabilization of the electrochemical interfaces and relies on an externally heated, hand-made tape cast

device[1] Initial tape cast platforms with screen printed metal oxide and Pt sensor electrodes have shown promising results but also clearly show the need for us to optimize the electrode and electrolyte compositions/morphologies and interfaces of these devices in order to demonstrate a sensitive, selective, and stable NO_x sensor. The information we are gathering via XCT and ESEM is valuable for achieving this objective. These sensors have been previously shown to be effective ammonia (NH_3) sensors[1].

Experimental

The sensors examined here were made using a tape-cast technique described in detail elsewhere.[18] The sensors consist of a platinum wire electrode and a lanthanum chromite ($La_{0.8}Sr_{0.2}CrO_3$) pellet electrode (from Praxair) embedded in a porous yttria-stabilized zirconia (YSZ) electrolyte. The YSZ electrolytes were tape cast from YSZ powders (Tosoh Tz-8Y). For response testing, the sensors were configured with the Pt electrode connected to the positive terminal of a Keithley 2400 source meter. Current bias was applied such that current flowed from the platinum electrode to the chromite electrode. The sensors were placed in a tube furnace with a flow of 200 sccm room air with the test gases mixed in.

Results and Discussion

Sensor Response

As reported previously[1], when this type of sensor is operated in a zero bias mode, it behaves as a hydrocarbon (HC) sensor with a positive interference from NO and a negative interference from NO_2. Operating the sensor in a negative current bias mode yields a positive voltage response for all the gases including NO, NO_2, and HCs. The sensor can be optimized for detection of NO_x by operating it an appropriate positive `current bias, which yields a large response to NO_x with very little interference from hydrocarbons (Fig. 1).

The sensor for which response is demonstrated in Figs. 1 and 2 was sintered at 1100 °C using a procedure described elsewhere[18]. Fig. 1 displays the response of the sensor to NO, NO_2, C_3H_6 (propene), and C_3H_8 (propane) with no bias and with a +0.6 μA current bias, when the sensor was operated at 517 °C. With the applied current bias an almost identical response of ~50 mV/100 ppm to both NO and NO_2 is observed with an almost negligible response to the two hydrocarbon species (~0.8 mV/100 ppm for C_3H_6 and ~0.4 mV/100 ppm for C_3H_8). With no bias there is a small response to the NO_x species (1 mV/100 ppm for NO and 4 mV/100 ppm for NO_2) and a larger response for the HCs (~9 mV/100 ppm for both C_3H_6 and C_3H_8).

Response stability testing results of the sensor for NO_x are displayed in Fig. 2. The sensor was exposed to a sequence of various small concentrations of NO and then of NO_2, under three different current biases (+0.5 μA, +0.6 μA, +0.72 μA) at the same 517 °C operating temperature. NO and NO2 concentrations were ramped up from 0 to 100 ppm in 25 ppm increments and then back down to measure hysteresis and observe the return to the baseline voltage output. One can see that no significant hysteresis was observed in the response to either NO or NO_2. Closer inspection of the data in Fig. 2 reveals that the small shifts in the bias current around the optimized bias current do not have a significant effect on the absolute sensor voltage response level for a given concentration. This is an area which merits further study with the use of a dedicated reference electrode.

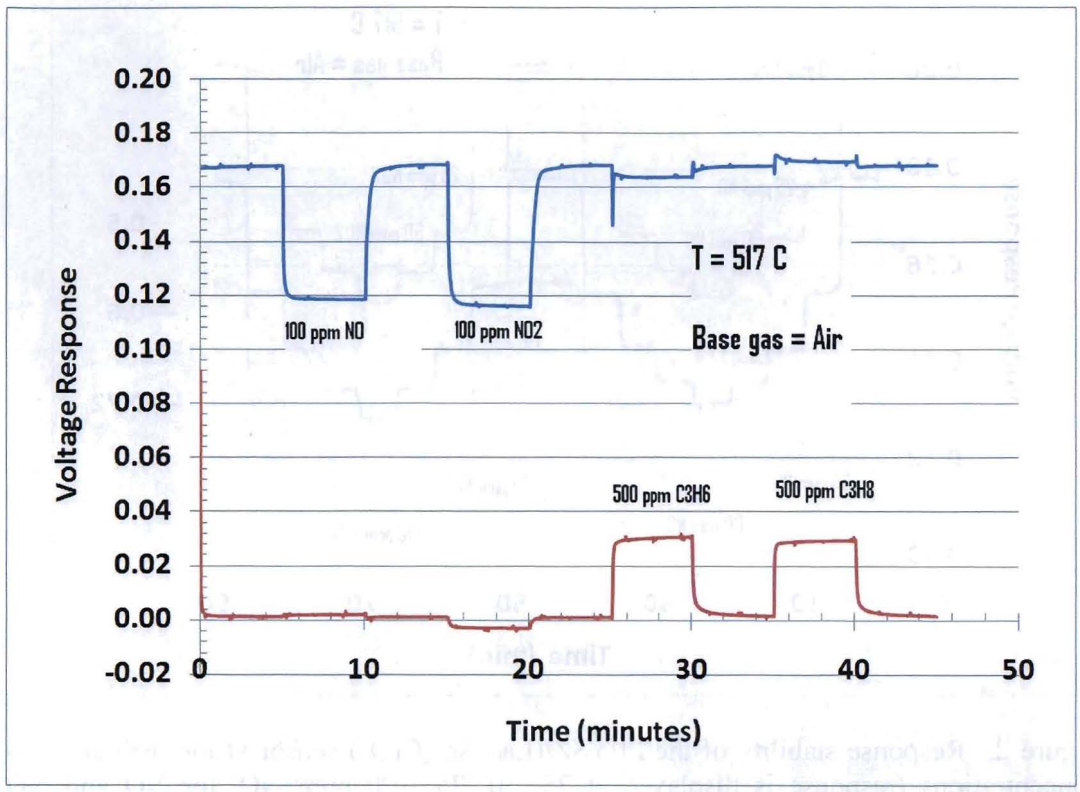

Figure 1. Response of a Pt/YSZ/($La_{0.8}Sr_{0.2}CrO_3$) sensor to various (100 ppm NO, 100 ppm NO_2, 500 ppm C_3H_6, 500 ppm C_3H_8) test gases; under zero bias (lower plot) and under a +0.6 μA current bias (upper plot). Sensor was operated in air at 517 °C.

.

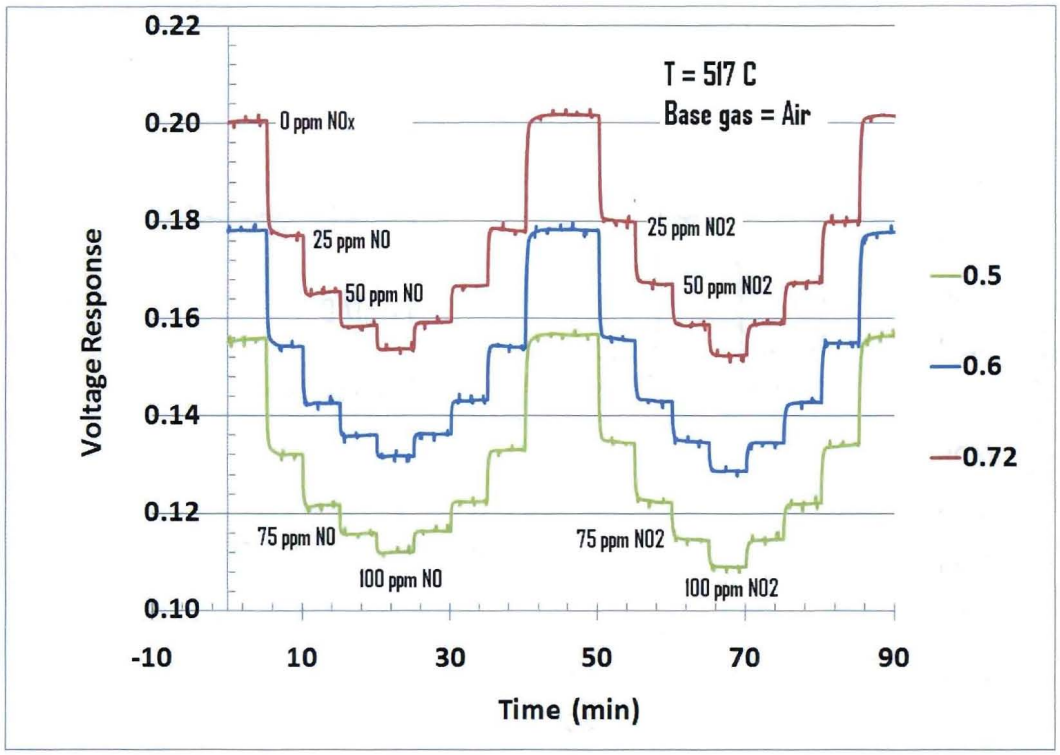

Figure 2. Response stability of the Pt/YSZ/($La_{0.8}Sr_{0.2}CrO_3$) sensor at low NO and NO_2 concentrations (response is displayed at 25, 50, 75, 100 ppm NO_x for NO and NO_2 consecutively) operated in air at 517 °C. Shown are plots of the response under 3 different current biases: +0.5 μA (lower plot), +0.6 μA(middle plot), and +0.72 μA(upper plot).

X-Ray Examination of Structure

The primary goal of using the X-ray tomography technique is to observe any defects in the electrolyte or in the electrolyte-electrode interfaces which may effect performance. Results of 90 keV X-ray examination of a sensor sintered at 1200 °C (Fig. 3) and of a "green body" sensor (a sensor prior to the sintering procedure, which still has plasticizers and binders present) are displayed (Figs 4 and 5). There are a significant amount of voids visible in the YSZ from gas bubbles, although our results seem to indicate that the sintering process reduces the density of such voids (compare Figs. 3 and 5.)

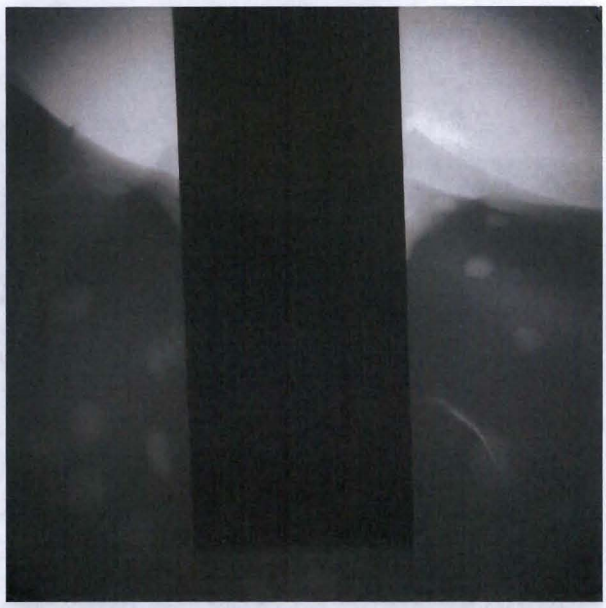

Figure 3. 90 keV X-ray Radiograph of Pt/YSZ/($La_{1-x}Sr_xCrO_3$) sensor sintered at 1200 °C showing the chromite electrode and gas bubbles in the YSZ.

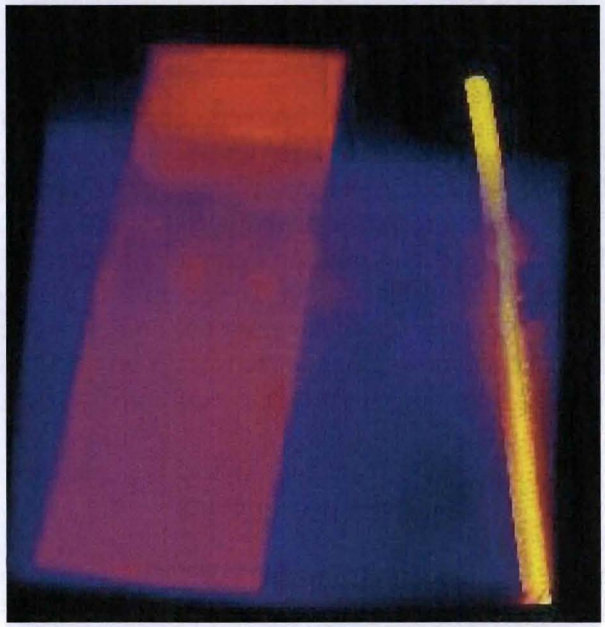

Figure 4. 3D image representation of a "green body" sensor based on a 90 keV X-ray tomography of Pt/YSZ/($La_{0.8}Sr_{0.2}CrO_3$) sensor prior to sintering showing the chromite electrode, Pt electrode, and gas bubbles in the YSZ.

Figure 5. 90 keV X-ray radiograph of a "green body" Pt/YSZ/($La_{1-x}Sr_xCrO_3$) sensor (prior to sintering) showing the Pt and chromite electrodes and gas bubbles in the YSZ.

Conclusions

A highly stable, sensitive NO_x sensor was observed under appropriate current bias from a LANL fabricated Pt electrode/YSZ electrolyte/($La_{0.8}Sr_{0.2}CrO_3$) electrode tape cast sensor, with a very high degree of response selectivity relative to propene and propane. The sensor exhibited a very similar response to both NO and NO_2. Interference from the hydrocarbons tested was negligible. X-ray tomography was used to examine electrolyte-electrode interface properties and electrolyte defects in this class of tape cast sensors. The effect of sintering temperature on sensor response and electrode-electrolyte interface and electrolyte bulk properties for this type of sensors is an area of current investigation, with these properties being investigated through use of both XCT and SEM.

Acknowledgments

We gratefully acknowledge funding from the US DOE Office of Office of Vehicle Technologies and Hydrogen Infrastructure Programs.

References

1. R. Mukundan, K. Teranishi, E. L. Brosha, and F. H. Garzon *J. Electrochem. Soc. Lett.* **10**, J26 (2007).
2. R. Mukundan, E. L. Brosha, F. H. Garzon, R. Novak, and R. Soltis, ECS Transactions **3** (10), 2006.
3. R. Mukundan, E.L. Brosha, F. Garzon, "Mixed Potential Sensors: From Understanding to Applications," ECS Transactions, 208th Meeting of the Electrochemical Society, Los Angeles, CA, (2005).

4. E. L. Brosha, R. Mukundan, R. Lujan, F. H. Garzon, *Sensors and Actuators B* **119**, 398 (2006).
5. F. H. Garzon, E. L. Brosha, and Rangachary Mukundan, *Solid State Ionics* **175,** 487 (2004)
6. R. Mukundan, E. L. Brosha, and F. H. Garzon, *J. Electrochem. Soc.* **150** (12) H2799-H284 (2003).
7. E. L. Brosha, R. Mukundan, D. R. Brown, F. H. Garzon, J. H. Visser, M. Zanini, Z. Zhou, and E. M. Logothetis, *Sensors and Actuators B* **69**, 171 (2000).
8. R. Mukundan, E. L. Brosha, D. R. Brown, and F. H. Garzon, *J. Electrochem. Soc.* **147** , 1583 (2000).
9. R, Mukundan, E. L. Brosha, D. R. Brown, and F. H. Garzon, *Electrochem. Solid-State Let.* **2** , 412(1999).
10. W. J. Flemming, *J. Electrochem. Soc.* **124** , 21 (1977) 21.
11. A. Vogel, G. Baier, and V. Schule, *Sensors and Actuators B* **15/16** , 147 (1993).
12. D.E. Williams, P. McGeehin, B.C. Tolfield, Proc. Second European Conference on Solid State Chemistry, Veldhoven, The Netherlands, June 7-9, p. 275 (1982).
13. H. Okamoto, H. Obayashi, and T. Kudo, *Solid State Ionics* **1**, 317 (1980).
14. P. T. Moseley *Solid State Gas Sensors* edited by P. T.Moseley and B. C. Tofield Adam Hilger p. 144 (1987).
15. R. Mukundan, E. L. Brosha, and F. H. Garzon, *US Patent # 6,605,202*, (2003).
16. R. Mukundan, E. L. Brosha, and F. H. Garzon, *US Patent # 6,656,336*, (2003).
17. F. H. Garzon, R. Mukundan, and E.L. Brosha, *US Patent # 7,264,700*, (2007).
18. R. Mukundan, E.L. Brosha, and F.H. Garzon, "Tape Cast Sensors and Method for Making," US Patent applied for Docket #104,887.